Pergamon

Solid State Communications, Vol. 103, No. 4, pp. 209–213, 1997
© 1997 Elsevier Science Ltd
Printed in Great Britain. All rights reserved
0038–1098/97 $17.00+.00

PII: S0038–1098(97)00178-6

NONMETAL–METAL–NONMETAL TRANSITION AND LARGE NEGATIVE MAGNETORESISTANCE IN (Ga, Mn)As/GaAs

A. Oiwa,[a,*] S. Katsumoto,[a] A. Endo,[a] M. Hirasawa,[a] Y. Iye,[a] H. Ohno,[b,†] F. Matsukura,[b] A. Shen[b] and Y. Sugawara[b]

[a]Institute for Solid State Physics, University of Tokyo, 7-22-1 Roppongi, Tokyo 106, Japan
[b]Research Institute of Electrical Communication, Tohoku University, Sendai 980-77, Japan

(*Received* 9 *April* 1997; *accepted* 25 *April* 1997 *by A. Okiji*)

We have studied magnetic and transport properties of a series of $Ga_{1-x}Mn_xAs$/GaAs samples with different Mn concentrations ($x = 0.015$–0.071). For Mn content higher than about 0.02, carrier(hole)-induced ferromagnetism is observed. Samples with $x = 0.035$ and 0.043 behave as ferromagnetic dirty metals. With further increase of Mn content above $x \sim 0.05$, the zero-field resistivity turns a semiconducting temperature dependence. Very large negative magnetoresistance is observed in nonmetallic samples near the metal-nonmetal transitions both in the low and the high Mn content regimes. © 1997 Elsevier Science Ltd

Keywords: A. semiconductors, magnetically ordered system, C. impurities in semiconductors, D. electronic transport.

Diluted magnetic semiconductors (DMSs) exhibit unique magnetic and transport properties which arise from the coupling of carrier spins and localized moments. Recent advent of III–V-compound-based DMSs such as $In_{1-x}Mn_xAs$ and $Ga_{1-x}Mn_xAs$ has opened a new area of research in the field of magnetic semiconductors [1–7]. Previous studies have revealed such interesting phenomena as carrier-induced ferromagnetic order [4, 5] and spin-dependent transport including anomalous Hall effect and negative magnetoresistance [1–3]. Introduction of magnetism into the III–V compounds has a great potential impact on both basic science and applications. In the past, studies of magnetic III–V compounds semiconductors have been hindered by the difficulties in the preparation of samples with high concentration of magnetic ions [8–11]. It has recently become possible to grow GaAs with magnetic impurity concentration much higher than before [8–11] (up to the order $\sim 10^{21}\ cm^{-3}$) by molecular beam epitaxy (MBE) employing a relatively low substrate temperature [6, 7].

In the present study, we prepared a series of $Ga_{1-x}Mn_xAs$/GaAs samples with different Mn contents and investigated their magnetic and transport properties. We focus our attention on low temperature magnetotransport properties and a metal–nonmetal transition as a function of the Mn content, x.

Samples used in the present study are listed in Table 1. Typical procedure for the MBE growth of (Ga, Mn)As/GaAs samples [6, 7] was as follows: First, a GaAs layer of thickness 100 nm was grown on a semi-insulating GaAs(1 0 0) substrate in a standard condition ($T_S \sim$ 700°C). Then, the substrate temperature was lowered to ~250°C and a 100 nm GaAs buffer layer and a 150 nm (Ga, Mn)As layer were successively grown. The low temperature growth was essential in avoiding surface segregation. The Mn content, x was estimated by an electron probe micro-analysis (EPMA). The lattice mismatch between the (Ga, Mn)As and GaAs layers ranges from ~0.1% to ~0.5% for $0.015 < x < 0.071$. It causes a compressive strain in the (Ga, Mn)As layer.

Magnetization measurements were carried out using a SQUID magnetometer in magnetic fields up to 5 T at temperatures from 2 K to 300 K. No trace of second phase MnAs was detected, which would be ferromagnetic with $T_C \sim 310$ K. The magnetic anisotropy of these

* To whom correspondence should be addressed.
† Also with Research Development Corporation of Japan (JRDC).

Table 1. Sample parameters. The values of the Curie temperature T_C were determined from the SQUID data

Sample	No. 1	No. 2	No. 3	No. 4	No. 5	No. 6
x	0.015	0.022	0.035	0.043	0.053	0.071
Conduction	Non-metal	Non-metal	Metal	Metal	Non-metal	Non-metal
Magnetism	Para	Ferro	Ferro	Ferro	Ferro	Ferro
T_C (K)	–	5	60	70	55	35

(Ga, Mn)As films was found to be such that the easy axis lies parallel to the film plane [6, 7]. Transport measurements were performed in magnetic fields up to 15 T applied perpendicular to the sample plane and at temperatures between 1.4 K and 300 K.

Figure 1 shows the temperature dependence of resistivity for the six samples listed in Table 1. Sample no. 1 with the lowest Mn content ($x = 0.015$) shows semiconducting behavior with an activation energy $\Delta \sim 75$ meV, which is comparable to a reported value of the ionization energy, ~110 meV for an isolated Mn acceptor in GaAs [8]. Sample no. 1 remains paramagnetic down to the lowest temperature (~1.5 K) of the present study. Sample no. 2 ($x = 0.022$) shows a similar temperature dependence of resistivity with an activation energy $\Delta \sim 40$ meV. This sample becomes ferromagnetic at low temperatures ($T_C \sim 5$ K). The critical value of x for the occurrence of ferromagnetism is thus between 0.015 and 0.022. With increasing Mn content, the system undergoes a nonmetal-to-metal transition. The critical Mn concentration lies between Sample no. 2 ($N_{Mn} = 4.8 \times 10^{20}$ cm^{-3}) and Sample no. 3 ($N_{Mn} = 7.7 \times 10^{20}$ cm^{-3}).

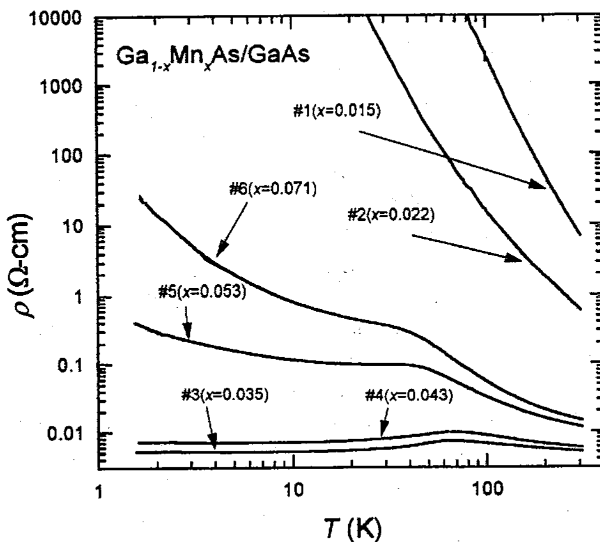

Fig. 1. Temperature dependence of resistivity for six samples of Ga$_{1-x}$Mn$_x$As/GaAs wity x ranging from 0.015 to 0.071.

Sample nos. 3 and 4 are classified as dirty metals. The ferromagnetic transition occurs at $T_C \sim 60$ and 70 K, respectively. These values of Curie temperature are much higher than those found in the (In, Mn)As system [3]. The temperature dependence of resistivity shows a peak around T_C. At temperatures much lower than T_C, the resistivity increases slightly with decreasing temperature as often found in dirty metals. The Hall resistivity of these samples contains a large contribution from the anomalous Hall effect [12], which makes estimate of carrier density difficult. Nevertheless, we can extract the ordinary Hall component by assuming the magnetization is saturated constant at the lowest temperature and the highest magnetic field and taking account of the magnetoresistance which enters into the anomalous Hall term. The hole density thus estimated turns out to be $p \sim 3–4 \times 10^{20}$ cm^{-3} for Sample no. 3 [6, 7].

Samples no. 5 ($x = 0.053$) and no. 6 ($x = 0.071$) with higher Mn content exhibit quite different transport behavior. The Curie temperature in these samples are $T_C \sim 55$ K and 35 K, respectively. A broad hump in the temperature dependence of resistivity around T_C is still seen in these samples. However, as temperature decreased below T_C the resistivity increases rapidly. Such "reentrant" non-metallic behavior of Sample nos. 5 and 6 suggests the strong localization of holes due to high degree of disorder in these samples. Since the Hall resistivity of these samples is dominated by a large anomalous Hall component, it is more difficult to extract information on the hole density than in the case of metallic samples.

The most drastic magnetoresistance effect occurs in the reentrant non-metallic regime. Figure 2(a) shows the magnetoresistance curves for Sample no. 6 at different temperatures. Magnetoresistance is negative at all temperatures investigated and its magnitude increases rapidly with decreasing temperature. At the lowest temperature (1.4 K), the resistivity at 15 T is diminished from its zero-field value by more than two orders of magnitude.

Fairly large negative magnetoresistance is also seen in Sample no. 2, although the measurement is limited to high temperature range. On the other hand, the resistivity of Sample no. 1 is nearly independent of magnetic field.

The metallic samples, Samples nos 3 and 4, also

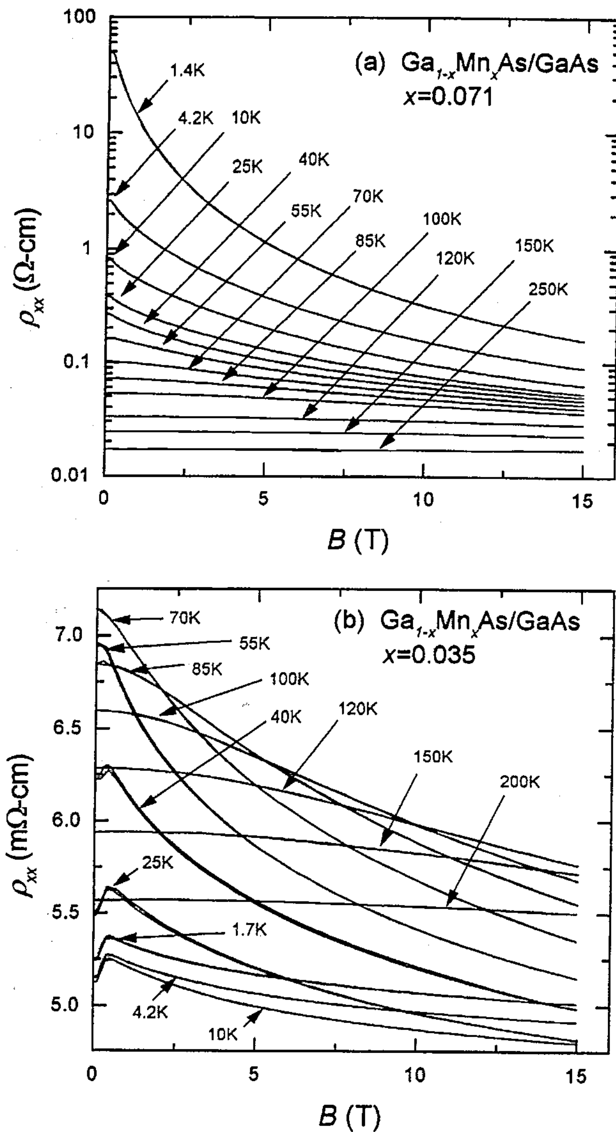

Fig. 2. (a) Magnetoresistance of Sample no. 6 (x = 0.071) at different temperatures ranging from 1.4 to 250 K. (b) Magnetoresistance of Sample no. 3 (x = 0.035) at different temperatures from 1.7 to 200 K.

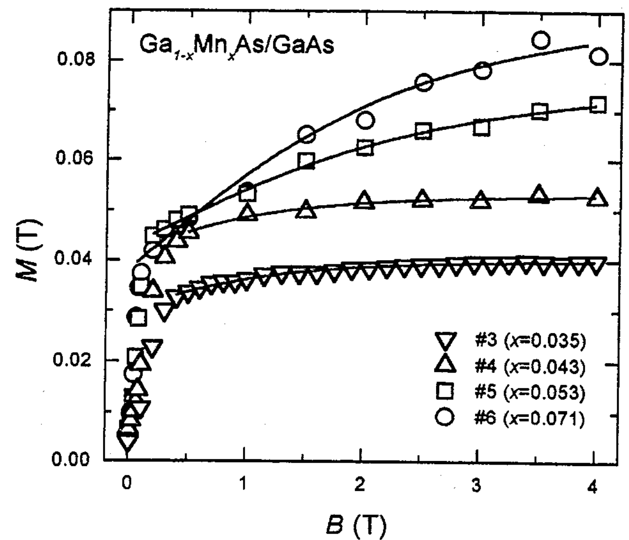

Fig. 3. Magnetization curves for four samples of $Ga_{1-x}Mn_xAs/GaAs$ with x ranging from 0.035 to 0.071 at 2 K. The solid curves are the fits of the modified Brillouin function to the experimental data. The magnetic field is applied perpendicular to the sample plane.

show negative magnetoresistance, but the magnitude is much smaller. Figure 2(b) shows the magnetoresistance curves for Sample no. 3. The decrease of resistivity is 25% at most even at 15 T. The negative magnetoresistance is the largest around T_C. A positive magnetoresistance emerges below T_C in the low field region.

In order to gain insight into the origin of the magnetoresistance, it is helpful to look into the magnetization data. Figure 3 shows magnetization curves for the four ferromagnetic samples with Mn content, x higher than 0.03 measured by SQUID at 2 K. Evidently, the magnetization of Sample nos. 5 and 6 in the reentrant non-metallic regime, do not reach saturation even at 4 T and keep increasing at higher fields. The magnetization curves are decomposed into two components. One is a ferromagnetic part which accounts for the low-field (<0.1 T) hysteresis loop and the other is the paramagnetic contribution which requires much higher field to saturate. Similar coexistence of ferromagnetic and paramagnetic moments has been observed earlier in the (In, Mn)As systems [3].

The slowly saturating component of magnetization can be represented by a Brillouin function modified by replacing the temperature T with $T + T_{AF}$ [18]. The parameter T_{AF} reflects the average strength of antiferromagnetic coupling between those Mn spins which do not participate in to the ferromagnetic component. The solid curves in Fig. 3 show the fit of the modified Brillouin function. Here, the Mn spin and the g-factor are assumed as 5/2 and 2, respectively. From this fit to Sample no. 6 the parameter T_{AF} is determined as 2.5 K, indicating a nearly paramagnetic character. The saturation value of the component represented by the modified Brillouin function in the high field limit is obtained as 0.056 T. The total saturation magnetization 0.093 T is close to the value 0.090 T calculated from $M_S = N_{Mn} g \mu_B S_{Mn}$. Therefore in Sample no. 6, for example, 40% of all Mn spins contribute to the ferromagnetic component and the remaining 60% behave as nearly paramagnetic spins.

Such a slowly saturating component of magnetization is also observed in the metallic samples (nos. 3 and 4) though they are smaller in magnitude. For Sample no.

3, the slowly saturating component is about 20%. As seen in Fig. 3, the slowly saturating component increases with increasing Mn content, while the ferromagnetic one remains roughly constant. These observations seem to indicate that the spatial inhomogeneity in the Mn distribution in a mesoscopic scale increases with increasing Mn content.

Let us now discuss the origin of the magnetoresistance. We begin with the metallic regime. Here, the basic picture is that holes of the density on the order of 10^{20} cm^{-3} in the valence band are scattered mainly by the Mn impurities. The resistivity peak around T_C can be attributed to critical scattering [13, 14], namely, carrier scattering by fluctuating local magnetic moments. Matsukura *et al.* [15] analyzed the magnetoresistance in the paramagnetic region above T_C in terms of the spin disorder scattering model [16, 17] to obtain a good fit. The magnetoresistance at low temperatures appears to consist of two components. The positive component occurs below T_C and in the low field range. The positive component disappears when the magnetic field is applied parallel to the film plane, i.e., parallel to the easy axis of magnetization [15]. Therefore it is natural to attribute this positive component to the so-called anisotropic magnetoresistance effect often seen in ferromagnetic metals. by contrast, the negative component persists well above the field range of ferromagnetic hysteresis loop and is observed both above and below T_C. Thus, the negative component is associated with the slowly saturating component of magnetization.

As for the large negative magnetoresistance in the non-metallic regime, we present two types of possible scenarios. The first is a polaronic picture. In magnetic semiconductors, a charged carrier is likely to form a bound magnetic polaron, i.e. a composite of the carrier and surrounding cloud of Mn spins polarized via p–d exchange interaction [19]. At zero field, the magnetic polarons have to move through a sea of Mn spins, which are more or less randomly oriented. Their motion, therefore, involves flipping many Mn spins, making the polarons massive and immobile. With increasing magnetic field, all Mn spins are progressively aligned to the direction of the applied magnetic field, which makes the holes increasingly mobile. In this picture, the negative magnetoresistance is attributed to smearing of the polaronic cloud with increasing magnetic field [20] and it is correlated with the slowly increasing part of magnetization in the high field region.

The second picture is based on Anderson localization. In an Anderson localized system, the Fermi level is located on the localized side of the mobility edge. Applied magnetic field causes the Zeeman shift of the mobility edge relative to the Fermi energy. For one of the spin subbands, the mobility edge moves toward the Fermi level, while it moves away for the other spin subband. This gives rise to a negative magnetoresistance because of the exponential dependence of the wave function overlap on the localization length $\xi \propto (\epsilon_C - \epsilon)^{-\nu}$, where ϵ_C is the mobility edge and ϵ is the energy of the localized state. ν is an exponent on the order of unity [21]. In the case of DMSs, one may expect this effect to be enhanced in two ways. Firstly, an enhanced g-factor gives rise to a large Zeeman shift. Secondly, the randomness itself can change with magnetic field due to the alignment of moments. Hence, the mobility edge is also a function of magnetic field.

In summary, we have observed a nonmetal-metal-nonmetal transition in $Ga_{1-x}Mn_xAs$/GaAs system as a function of the Mn content, x. In the metallic samples, the magnetoresistance at temperatures above T_C is governed by the spin disorder scattering. In the semiconducting samples near the metal-nonmetal transition, large negative magnetoresistance has been observed. Magnetization measurements have revealed a slowly saturating component in addition to a ferromagnetic component. The former is considered to be responsible for the negative magnetoresistance observed at lower temperatures. We have presented two-types of scenarios for the large negative magnetoresistance, a magnetic polaron model and an Anderson localization model.

Acknowledgements—This work is partly supported by a Grant-in-Aid for the Scientific Research from the Ministry of Education, Science, Sports and Culture, Japan. The authors thank Professor H. Takagi at ISSP for his help with the SQUID measurements.

REFERENCES

1. Munekata, H., Ohno, H., von Molnar, S., Segmüller, A., Chang, L.L. and Esaki, L., *Phys. Rev. Lett.*, **63,** 1989, 1849.
2. Munekata, H., Zaslavsky, A., Fumagalli, P. and Gambino, R.J., *Appl. Phys. Lett.*, **63,** 1993, 2929.
3. Ohno, H., Munekata, H., Penny, T., von Molnar, S. and Chang, L.L., *Phys. Rev. Lett.*, **68,** 1992, 2664.
4. Munekata, H., Penny, T. and Chang, L.L., *Surf. Sci.*, **267,** 1992, 342.
5. Koshihara, S., Oiwa, A., Katsumoto, S., Hirasawa, H., Iye, Y. and Munekata, H., Submitted.
6. Ohno, H., Shen, A., Matsukura, F., Oiwa, A., Endo A., Katsumoto, S. and Iye, Y., *Appl. Phys. Lett.*, **69,** 1996, 363.
7. Matsukura, F., Oiwa, A., Shen, A., Sugawara, Y., Akiba, N., Kuroiwa, T., Ohno, H., Endo, A., Katsumoto, S. and Iye, Y., *Appl. Surf. Sci.* (to be published).
8. Chapman, R.A. and Hutchinson, W.G., *Phys. Rev. Lett.*, **18,** 1967, 443.
9. Woodbury, D.A. and Blakemore, J.S., *Phys. Rev.*, **B8,** 1973, 3803.
10. Andrianov, D.G., Bol'sheva, Yu.N., Lazareva,

G.V., Savel'ev, A.S. and Yakubenya, S.M., *Fiz. Tekh. Poluprovodn.*, **17,** 1983, 810 [*Sov. Phys. Semicond.*, **17,** 1983, 506].

11. Mac, W., Twardowski, A. and Hennel, A.M., in *Proc. 11th Int. Conf. Phys. Semicond.*, Vancouver, 1994 (Edited by D.J. Lockwood), p. 2569. World Scientific, 1995.
12. Hurd, C.M., *The Hall Effect and Its Applications* (Edited by C.L. Chein and C.R. Westgate), p. 43. Plenum, 1980.
13. de Gennes, P.G. and Friedel, J., *J. Phys. Chem. Solids*, **4,** 1958, 71.
14. Fisher, M.E. and Langer, J.S., *Phys. Rev. Lett.*, **20,** 1968, 665.
15. Matsukura, F., Shen, A., Sugawara, Y., Ohno, Y. and Ohno, H., Unpublished.
16. Allen, S.J. Jr., Tabatabaie, N., Palmstrom, C.J., Hull, G.W., Sands, T., DeRosa, F., Gilchrist, H.L. and Garrison, K.C., *Phys. Rev. Lett.*, **62,** 1989, 2309.
17. Kasuya, T., *Prog. Theor. Phys.*, **16,** 1956, 58.
18. Heiman, D., Shapira, Y., Foner, S., Khazai, B., Kershaw, R., Dwight, K. and Wold, A., *Phys. Rev.*, **B29,** 1984, 5634.
19. Wolff, P.A., in *Semiconductors and Semimetals*, **25,** "Diluted Magnetic Semiconductors" (Edited by J.K. Furdyna and J. Kossut), p. 413. Academic Press, 1988.
20. von Molnar, S., Flouquet, J., Holtzberg, F. and Remenyi, G., *Phys. Rev. Lett.*, **51,** 1983, 706 and *Solid State Electron*, **28,** 1985, 127.
21. Fukuyama, H. and Yosida, K., *J. Phys. Soc. Japan*, **46,** 1979, 102.